### ORIGINAL RESEARCH

# The Role of SHP2 in Advancing COPD: Insights into Oxidative Stress, Endoplasmic Reticulum Stress, and Pyroptosis

Haidong Ding, MD; Rina Wu, MM

#### **ABSTRACT**

**Background** • Chronic Obstructive Pulmonary Disease (COPD) is characterized by airflow limitation and inflammation resulting from genetic and environmental factors, notably cigarette smoke. Pyroptosis, a cell death process, is implicated in COPD, but its mechanisms are unclear. SHP2, a phosphatase, modulates inflammatory pathways, suggesting a role in COPD pathogenesis and potential therapeutic avenues.

**Objective** • This study investigates the mechanism by which SHP2 regulates cell pyroptosis in bronchial epithelial cells in COPD patients.

**Methods** • In this prospective study, we employed *in vivo* and *in vitro* models to investigate the mechanisms underlying COPD progression. Hematoxylin and eosin (H&E) staining were utilized to assess the morphological changes characteristic of COPD. Electron microscopy enabled precise quantification of pyroptotic bodies to highlight cellular changes associated with COPD pathogenesis. Immunofluorescence analysis facilitated the measurement of protein fluorescence intensity, allowing for the assessment of inflammatory responses within bronchial epithelial cells. Additionally, Western blot

analysis was conducted to evaluate the expression levels of key pathway proteins involved in COPD progression.

Results • In the COPD model, lesions worsened in SHP2-KD mice compared to SHP2-NC. Western blot results showed increased p22, p47, p-IRE1 $\alpha$ , XBP1, STING, p-TBK1, NLRP3, Caspase1, and IL-1 $\beta$  expression levels in both *in vivo* and *in vitro* models. Transmission electron microscopy revealed more pyroptotic bodies in SHP2-KD+CSE than in SHP2-NC+CSE. Immunofluorescence demonstrated significantly higher NLRP3 and GSDMD fluorescence intensities in SHP2-KD+CSE versus SHP2-NC+CSE. Additionally, Western blot analysis indicated increased expression of Bax, Caspase3, Caspase8, and Caspase9 proteins in the *in vitro* model. No differences were observed between SHP2 NC and SHP2-KD groups without CSE stimulation in immunofluorescence, electron microscopy, and Western blot findings in the cellular model.

**Conclusions** • SHP2 promotes COPD progression by inducing oxidative stress, endoplasmic reticulum stress, and pyroptosis. (*Altern Ther Health Med.* [E-pub ahead of print.])

Haidong Ding, MD, Department of Pulmonary and Critical Care Medicine; Affiliated Hospital of Inner Mongolia University for the Nationalities; Inner Mongolia; China. Rina Wu, MM, Endocrinology Department; Affiliated Hospital of Inner Mongolia University for the Nationalities; Inner Mongolia; China.

Corresponding author: Rina Wu, MM E-mail: wurina223@126.com

### INTRODUCTION

Chronic obstructive pulmonary disease (COPD) manifests as irreversible airflow obstruction and airway inflammation primarily attributed to smoking.<sup>1</sup> Cigarette Smoke Extract (CSE), a significant constituent of tobacco

extract, induces its effects via oxidative stress and signal transduction pathways.<sup>2</sup> Reactive oxygen species (ROS) are intricately associated with exposure to environmental pathogens and toxins.<sup>3</sup> CSE contributes to pulmonary inflammation by modulating gene expression profiles.<sup>4</sup>

There is a well-established association between CSE and COPD, with CSE accumulating and concentrating in the lungs, thereby stimulating human bronchial epithelial (HBE) cells. Pyroptosis, an essential process in tissue inflammation triggered by CSE, could play a crucial role in driving the progression of COPD. Cellular pyroptosis, which relies on the activation of the Nucleotide-binding oligomerization domain (NOD)-like receptor protein 3 (NLRP3) inflammasome and caspase-1, leads to the buildup of mature Interleukin-1 beta (IL-1 $\beta$ ). This process is notably involved in pulmonary diseases.

Protein tyrosine phosphatase 2 (SHP2), which contains Src homology 2 (SH2) domains, represents a widely expressed non-receptor protein tyrosine phosphatase (PTP).<sup>8</sup> The human PTPN11 gene encodes the SHP2 protein's N-SH2 and C-SH2 domains critical for its subcellular localization. The PTP domain is also essential for its enzymatic activity.<sup>9</sup> SHP2 has been recognized for its pivotal role in cell proliferation and differentiation and its responsiveness to growth factors and cytokines.<sup>10</sup>

SHP2 is implicated in modulating the NLRP3 inflammasome, potentially impacting the signaling pathway associated with cell pyroptosis. It may play a role in inhibiting NLRP3 inflammasome activation to mitigate cell pyroptosis. Studies indicate that SHP2 negatively regulates interferon (IFN)- $\beta$  production in macrophages upon Toll-like receptor (TLR) 3 and TLR4 activation. Recent research suggests a regulatory role for SHP2 in the NLRP3 inflammasome.<sup>11</sup>

Our study explored how SHP2 modulates NLRP3-mediated cell pyroptosis, aiming to identify therapeutic targets for managing COPD progression. Our findings contribute to understanding SHP2's impact on inflammatory pathways, offering significant promise for developing targeted interventions to alleviate the burden of COPD on patients' respiratory health.

### **MATERIALS AND METHODS**

### **Study Design**

The study employed a murine model to investigate the development of COPD induced by lipopolysaccharide (LPS) intranasal administration and cigarette smoke exposure. A total of 10 specific pathogen-free (SPF) male mice, aged 6 to 8 weeks, underwent adaptive breeding in an SPF-level animal laboratory. The mice were subjected to controlled conditions with ad libitum access to food and water throughout the experiment. COPD was induced through exposure to cigarette smoke for 1 hour twice daily, complemented by LPS administration. The successful establishment of the COPD model was determined by observing physical manifestations indicative of respiratory distress.

### **Animal Rearing and Model Establishment**

**Housing Conditions.** A total of 10 SPF male mice, aged 6 to 8 weeks, underwent adaptive breeding for one week in an SPF-level animal laboratory maintained at a relative humidity of 45% and a temperature of  $(25\pm2)^{\circ}$ C. The animals had ad libitum access to food and water throughout the experiment.

**Model Induction.** The establishment of a COPD mice model involved intranasal administration of LPS and exposure to cigarette smoke. Mice were housed in a smoking chamber, where they were exposed to smoke from 10 cigarettes for 1 hour twice daily, in the morning and evening, with a 6-hour interval between sessions, six days per week, over a period of 30 days. Successful modeling was indicated by observed indicators such as lackluster fur, partial alopecia, agitation, clustering during smoke exposure, lethargy, curled-up rest, perspiration, abdominal distention, rapid breathing, head nodding

movements, and in severe cases, overt mouth-breathing.

**Virus Administration Protocol.** Our laboratory generated AVV8-SHP2-KD lentivirus and AVV8-SHP2-NC empty vector constructs on the established model. Six mice were allocated to each group. On day 20, when the mice exhibited clear signs of illness, lentivirus infection was administered. Mice were restrained using a fixator, and their tails were immersed in warm water at approximately 40°C. Subsequently, a syringe was used to draw the virus at a dose of 10<sup>7</sup> per mouse, which was then placed on ice for later use.

Once the tail veins of the mice were engorged, any remaining drops of water were removed with a dry cotton ball. An injection was administered in the distal third of the tail vein, and if resistance was encountered during the procedure, it was halted. After a successful injection, a dry cotton ball was applied to the injection site for 10 seconds to ensure hemostasis, and the site was disinfected with an alcoholic cotton ball to prevent infection. On the 30th day, the mice were euthanized, and following dissection, their lungs were excised and fixed with paraformaldehyde.

### Hematoxylin and Eosin (H&E) Staining Protocol

Samples were initially fixed with 4% paraformaldehyde, followed by dehydration in an ethanol gradient and subsequent embedding in paraffin. Paraffin blocks were then sectioned to a thickness of 5µm. Hematoxylin staining was performed for 10 minutes, followed by differentiation in 1% hydrochloric alcohol for 10 minutes and treatment with 0.05% lithium carbonate bluing for 3 seconds. Finally, samples were stained with eosin for 5 minutes and examined under an inverted microscope.

### **Cell Culture and Experimental Transfection Procedures**

Cell Culture and Transfection. Human bronchial epithelial-like cells (16HBE) were procured from Shanghai Zhong Qiao Xin Zhou Biotechnology Co., Ltd. These cells were cultured in an L15 medium supplemented with 10% fetal bovine serum (FBS) and 1% penicillin-streptomycin. Upon reaching the logarithmic growth phase, the cells were digested, centrifuged, resuspended, and evenly seeded onto 6-well plates at a 2.0  $(\pm 0.2) \times 10^5$ /mL density, with 2 mL of complete culture medium per well. The cells were then cultured for 24 hours.

**Transfection Protocol.** After 24 hours, when the cells reached 70%-80% confluency, the old culture medium was aspirated, and 2 mL of fresh complete culture medium was added. Four sterile enzyme-free 1.5 mL Eppendorf tubes were prepared, each containing 125  $\mu L$  of serum-free, double-antibiotic-free DMEM high sugar culture medium pre-warmed to 37°C. AVV8-SHP2 lentiviruses and the AVV8 empty vector were employed to transfect cells with SHP2 NC and SHP2 KD, both in the presence and absence of CSE treatment.

Following enzymatic digestion with trypsin, the cells were seeded into 6-well plates. After overnight incubation, when the cell density reached 50%-80%, the cells were washed twice with phosphate-buffered saline (PBS), and

experiments were divided into four groups: SHP2 NC, SHP2 KD, SHP2 NC+CSE, and SHP2 KD+CSE. Subsequently, the medium containing serum was replaced, and the cells were further cultured for 48 hours.

### Western Blot Analysis

Tissue proteins were obtained by grinding tissue samples in liquid nitrogen and collecting them in 1.5 mL centrifuge tubes, while cell samples were scraped off the plate and collected in similar tubes. Samples were lysed for 30 minutes in RIPA buffer containing phosphatase and protease inhibitors. The protein concentration was determined using the bicinchoninic acid (BCA) method. Subsequently, all samples were denatured by heating at 95°C for 5 minutes and subjected to 10% SDS-PAGE electrophoresis under 120V.

Proteins were then transferred onto PVDF membranes, which were blocked with fat-free milk at room temperature for 60 minutes and incubated overnight at 4°C with primary antibodies against p-IRE1 $\alpha$  (1:1000), P22 (1:1000), P47 (1:1000), SHP2 (1:1000), p-SHP2 (1:1000), XBP-1 (1:1000), STING (1:1000), p-TBK1 (1:1000), NLRP3 (1:1000), Caspase1 (1:1000), IL-1 $\beta$  (1:1000), GSDMD (1:1000), Caspase3 (1:1000), Caspase8 (1:1000), and Caspase9 (1:1000). Membranes were then incubated for 2 hours at room temperature with a secondary antibody (1:1000). Following a wash with PBS, protein bands were visualized using ECL reagents and exposed on a Tanon 5200 instrument.

### Immunofluorescence Assay

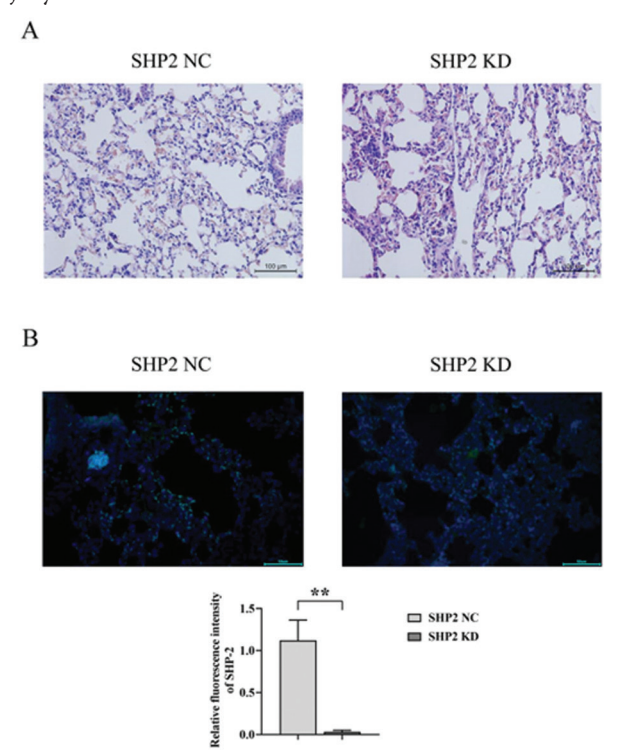
Slides were prepared, and cells were digested with trypsin to obtain a single-cell suspension. Subsequently, slides were carefully placed in a sterilized culture dish, followed by the addition of the single-cell suspension onto the slides. The culture dish was then incubated at 37°C with 5% CO<sub>2</sub>. After three washes with  $37^{\circ}$ C PBS, the samples were fixed with polyformaldehyde for 15 minutes.

The slides were washed three times with PBS, with each wash lasting 3 minutes. A sufficient amount of diluted SHP2 (1:1000), NLRP3 (1:1000), and GSDMD (1:1000) monoclonal antibody was added to each slide and incubated in a wet box at 4°C overnight. Subsequently, the slides were washed three times with PBS, with each wash lasting 3 minutes. At room temperature, the fluorescent secondary antibody was added to the slides and incubated for 30 minutes. Slides were once again washed three times with PBS for 5 minutes each and observed under a fluorescence microscope.

### **Transmission Electron Microscopy Procedure**

The 16HBE cell was fixed using a 2.5% paraformaldehyde solution. Subsequently, the uranyl acetate solution was dropped onto a copper grid with a pipette, covered with a wax dish, and stained for 30 minutes. After rinsing, the copper grid was washed three times with distilled water, dried with filter paper, and allowed to air dry. Lead citrate staining was performed by placing the washed and dried copper grid into another wax dish containing a few grains of

**Figure 1.** The Impact of SHP2 Knockdown on Pathological Injury in COPD



Note: Figure 1 A: Hematoxylin and eosin (H&E) staining comparing SHP2 NC and SHP2 KD groups. Figure 1B: Immunofluorescence staining of SHP2 and statistical analysis in SHP2 NC and SHP2 KD groups. n=6, vs. SHP2 NC group, \*P < .05, \*\*P < .01.

solid sodium hydroxide to absorb  $\mathrm{CO}_2$  and prevent lead carbonate formation. Lead citrate staining solution was then dropped onto the copper grid, the dish was sealed, and after staining for 15 minutes, the copper grid was removed, washed three times with water, dried with filter paper, and air-dried before observation. The observation was conducted using a Libra200 projection electron microscope.

### **Statistical Analysis**

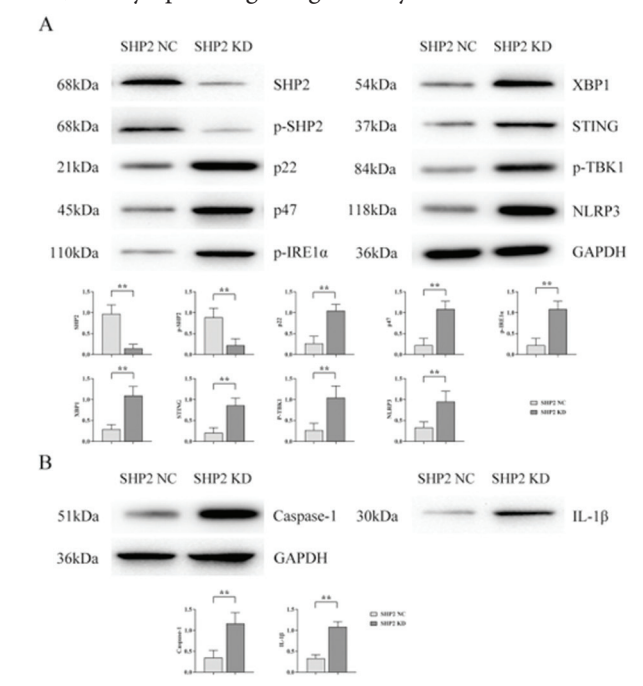
Data analysis was conducted utilizing SPSS 25.0 (International Business Machines, Corp., Armonk, NY, USA). Quantitative data were presented as mean values with corresponding standard deviations ( $\bar{x} \pm s$ ). Intergroup differences were assessed through the t test, while count data were represented as percentages [n (%)] and analyzed using the chi-squared test. A significance level of P < .05 indicated statistical significance.

### **RESULTS**

# Effect of SHP2 Knockdown on Pulmonary Pathological Damage in a Mice Model of COPD

We induced a mice model of COPD and subsequently administered AVV8-SHP2 KD and AVV8-SHP2 NC via the tail vein to the established model mice, dividing them into two groups: the SHP2 NC group and the SHP2 KD group, each comprising five mice. Lung tissues were then collected for H&E staining, revealing successful model construction

**Figure 2.** Impact of SHP2 Knockdown on Oxidative Stress, ER Stress, and Pyroptosis Signaling Pathway Proteins in COPD Mice



Note: Figure 2A: Western blot analysis showing protein expression levels of p22, p47, p-IRE1 $\alpha$ , XBP1, STING, p-TBK1, and NLRP3 in each group of COPD mice, along with statistical analysis. Figure 2B: Western blot analysis demonstrating protein expression levels of caspase-1 and IL-1 $\beta$  in each group, accompanied by statistical analysis. The sample size for each group was 6; comparisons were made against the SHP2 NC group, \*P < .05, \*\*P < .01.

characterized by thickened bronchial walls, inflammatory cell infiltration around the airways, widened alveolar septa with inflammatory cell infiltration, and compensatory expansion of alveolar spaces.

Furthermore, H&E staining demonstrated a more severe inflammatory phenotype in the COPD mice lung tissue of the SHP2 KD group compared to the SHP2 NC group, refer to Figure 1A. Immunofluorescence staining revealed a decrease in SHP2 immunofluorescence intensity in the lung tissue of the SHP2 KD group compared to the SHP2 NC group, refer to Figure 1B.

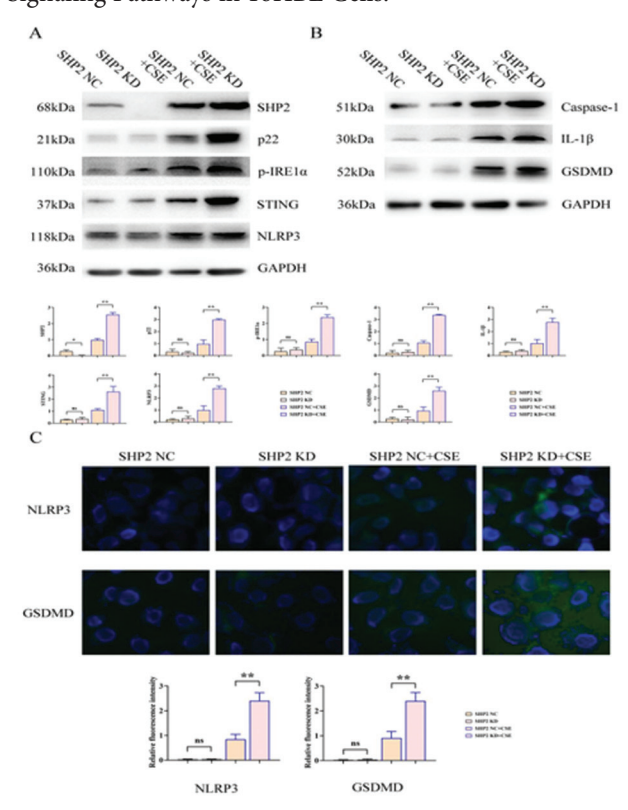
### Effect of SHP2 Knockdown on Protein Expression in Mice with COPD

Previous literature has revealed a significant association between SHP2 and oxidative stress, ER stress, and cell pyroptosis. Subsequent Western blot analysis revealed a marked reduction in the SHP2 and p-SHP2 protein levels in the SHP2 KD group compared to the SHP2 NC group. Concurrently, the levels of p22, p47, p-IRE1 $\alpha$ , XBP1, STING, p-TBK1, NLRP3 (Figure 2A), Caspase1, and IL-1 $\beta$  (Figure 2B) exhibited a notable increase in the SHP2 KD group.

# Effect of SHP2 Knockdown on Protein Expression in 16HBE Cells Exposed to CSE

Building upon the findings from *in vivo* experiments demonstrating the role of SHP2 knockdown in elevating oxidative stress, ER stress, and pyroptosis-related proteins,

**Figure 3.** The Impact of SHP2 Knockdown on Proteins Involved in the Oxidative Stress, ER Stress, and Pyroptosis Signaling Pathways in 16HBE Cells.



Note: Figure 3A: Western blot analysis of SHP2, p22, p47, p-IRE1 $\alpha$ , STING, and NLRP3 protein expression levels in SHP2 NC + CSE, SHP2 KD + CSE, SHP2 NC, and SHP2 KD groups, with accompanying statistical analysis. Figure 3B: Western blot analysis of caspase-1, IL-1 $\beta$ , and GADMD protein expression levels in each group, along with statistical analysis. Figure 3C: Immunofluorescence detection and statistical analysis of NLRP3 and GSDM expression levels in each SHP2 NC + CSE, SHP2 KD + CSE, SHP2 NC, and SHP2 KD groups. n=3 indicates a sample size of three for each group. \*P < .05, \*\*P < .01 compared to the SHP2 NC + CSE group.

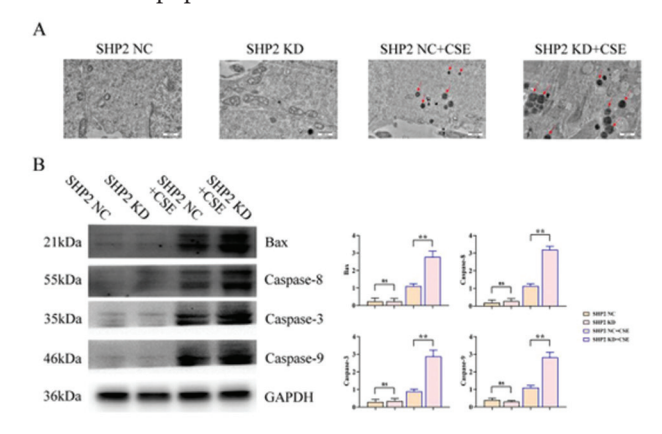
we conducted *in vitro* investigations. 16HBE cells were infected with adenovirus and concurrently exposed to CSE, leading to the categorization of cell experiments into four groups: SHP2 NC group, SHP2 KD group, SHP2 NC+CSE group, and SHP2 KD+CSE group.

Western blot analysis revealed a significant upregulation of SHP2, p22, p47, p-IRE1 $\alpha$ , STING, NLRP3, Caspase1, IL-1 $\beta$ , and GSDMD in the SHP2 KD+CSE group compared to the SHP2 NC+CSE group. However, there were no changes in these protein levels without CSE stimulation, refer to Figures 3A and 3B. Furthermore, immunofluorescence results demonstrated a notable increase in the fluorescence intensity of NLRP3 and GSDMD in the SHP2 KD+CSE group relative to the SHP2 NC+CSE group, while no change was observed in fluorescence intensity without CSE stimulation, refer to Figure 3C.

### Impact of SHP2 Knockdown on Pyroptotic Body Formation and Apoptotic Protein Levels in 16HBE Cells

Both *in vivo* and *in vitro* findings have collectively demonstrated that SHP2 knockdown induces cell pyroptosis.

**Figure 4.** The Impact of SHP2 Knockdown on Pyroptotic Bodies and Apoptosis in 16HBE Cells.



Note: Figure 4A: Detection of Pyroptotic Body Formation Using Transmission Electron Microscopy in SHP2 NC + CSE, SHP2 KD + CSE, SHP2 NC, and SHP2 KD Groups. Figure 4B: Western blot analysis of Bax, Caspase-3/8/9 protein expression levels in each group, with accompanying statistical analysis. n=3, a sample size of three for each group. \*P < .05, \*\*P < .01 compared to the SHP2 NC + CSE group.

Given that pyroptosis generates apoptotic bodies within cells, transmission electron microscopy results revealed a notable increase in the number of apoptotic bodies in the SHP2 KD+CSE group compared to the SHP2 NC+CSE group, while no change was observed without CSE stimulation, refer to Figure 4A.

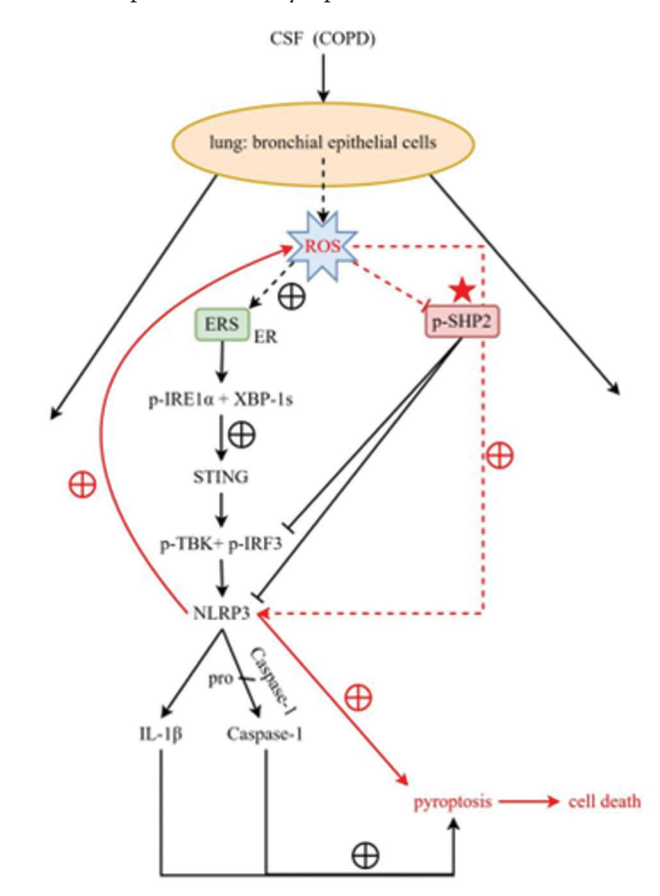
Subsequently, we conducted a Western blot analysis to assess alterations in apoptotic-related proteins consequent to cell pyroptosis. The results demonstrated a significant upregulation of Bax, Caspase3, Caspase8, and Caspase9 in the SHP2 KD+CSE group relative to the SHP2 NC+CSE group. However, there was no change in these protein levels without CSE stimulation, refer to Figure 4B.

# Schematic Diagram of SHP2 Regulation in Bronchial Epithelial Cell Pyroptosis in COPD

We developed a schematic diagram that depicts the pivotal role of SHP2 in modulating bronchial epithelial cell pyroptosis in COPD. In the context of our findings, SHP2 knockdown exacerbates pyroptosis, as evidenced by increased formation of pyroptotic bodies and elevated expression of pyroptosis-related proteins such as NLRP3, Caspase1, and IL-1 $\beta$ . These alterations are further associated with enhanced oxidative stress and endoplasmic reticulum stress, contributing to the progression of COPD.

Figure 5 shows that COPD can induce ERS in the lung bronchial epithelial cells, which can activate the IRE1 $\alpha$ -XBP-1s pathway and the STING-TBK1-IRF3 pathway. These pathways can increase the expression of NLRP3 and proIL-1 $\beta$ , which can form the inflammasome and activate caspase-1. Caspase-1 can induce pyroptosis and cell death and release IL-1 $\beta$  and IL-18, which can further amplify the inflammation and damage the lung tissue. The diagram also shows that some molecules, such as SHP2 and NOS2, can modulate or inhibit some of these pathways. This diagram suggests that

**Figure 5.** Schematic Diagram of SHP2 Regulation in Bronchial Epithelial Cell Pyroptosis in COPD.



Note: The diagram illustrates COPD-induced endoplasmic reticulum stress (ERS) in lung bronchial epithelial cells, activating the IRE1 $\alpha$ -XBP-1s and STING-TBK1-IRF3 pathways. These pathways elevate NLRP3 and proIL-1 $\beta$  expression, forming the inflammasome and activating caspase-1, leading to pyroptosis, cell death, and cytokine release, exacerbating lung tissue damage. Additionally, molecules like SHP2 and NOS2 can modulate or inhibit these pathways, suggesting SHP2 as a potential therapeutic target for mitigating pyroptosis-associated inflammation in COPD.

SHP2 can be a potential therapeutic target for mitigating pyroptosis-associated inflammation in COPD pathogenesis.

### **DISCUSSION**

CSE represents a primary source of exposure closely linked to pulmonary diseases. <sup>12</sup> Its detrimental effects include the development of lung tumors, inflammation, and airway hyperresponsiveness. <sup>1</sup> High concentrations of CSE exposure have been associated with cell apoptosis in lung epithelial cells. <sup>13</sup> Recent studies reveal that acute exposure to CSE alters the secretion profile of lung epithelial cells, resulting in the downregulation of proteins involved in wound healing and extracellular matrix organization. <sup>1</sup> Moreover, CSE induces an inflammatory response and cellular toxicity in human bronchial epithelial cells, manifested by an increased inflammatory cell population. <sup>2</sup>

In mice exposed to CSE, there is a concurrent increase in inflammatory cells and lung inflammatory cytokine concentrations. <sup>14</sup> Therefore, we conducted a study to

investigate the impact of CSE on the ROS/SHP2/NLRP3 signaling pathway in COPD bronchial epithelial cells. Previous studies have shown ROS production can prevent SHP2 inactivation and promote sustained SHP2 phosphorylation.<sup>11</sup> SHP2 acts as a negative regulator of NLRP3 inflammasome activation and can also activate NLRP3.<sup>15</sup> Furthermore, NLRP3 increases ROS production, a component of the ER stress response pathway.<sup>16</sup>

ROS initiates ER stress, a critical component of intracellular redox homeostasis. It has been shown that downstream of ER stress, IRE1 $\alpha$  and XBP-1s are phosphorylated. Activated IRE1 $\alpha$ +XBP-1s then stimulate the STING pathway, facilitating the phosphorylation of TBK1 downstream. TBK1, in turn, restrains the subsequent response of NLRP3 inflammasome activation. NLRP3 activation prompts the cleavage of procaspase-1, leading to the activation of caspase-1 and subsequent release of IL-1 $\beta$ , thereby inducing cell pyroptosis and accelerating cell apoptosis.

Our experiment validated the functionality of this pathway. Specifically, the knockdown of SHP2 impeded the progression of downstream pathways, including IRF3, TBK1, and NLRP3. Furthermore, NLRP3 facilitated ROS/ERS oxidative stress, while ROS/ERS heightened the activation of IRE1 $\alpha$ , XBP-1s, STING, TBK1, IRF3, and NLRP3 pathways. Consequently, NLRP3 increased the expression of caspase-1, IL-1 $\beta$ , and GADMD, thereby accelerating both cell pyroptosis and apoptosis.

These findings emphasize the pivotal role of SHP2 in modulating the ROS/ERS-mediated pathways implicated in COPD. Downregulating SHP2 activity effectively reduced the subsequent signaling pathways, notably impacting IRF3, TBK1, and NLRP3 cascades. Consequently, this suppression hindered both cell pyroptosis and apoptosis pathways. These results reveal SHP2 as a potential therapeutic target for managing COPD progression by regulating inflammatory responses and cell death pathways.

### **Study Limitations**

While our study sheds light on the complex pathways influenced by SHP2 knockdown in COPD, several limitations merit consideration. Firstly, the study primarily focused on cellular and murine models, limiting direct extrapolation to human subjects. Secondly, the duration of the experimental interventions may not fully capture the chronic nature of COPD progression. Additionally, while we explored key pathways, other molecular mechanisms may also contribute to COPD pathogenesis, warranting further investigation. Lastly, the complexity of cellular interactions and signaling pathways underscores the need for comprehensive multiomic analyses to explain the complete landscape of SHP2 involvement in COPD.

### CONCLUSION

In conclusion, our study reveals a critical role for SHP2 in modulating key signaling pathways implicated in COPD pathogenesis. Knockdown of SHP2 mitigated downstream

cascades associated with cell pyroptosis and apoptosis, suggesting its potential as a therapeutic target. These findings highlight the intricate relationship between oxidative stress, ER stress, and inflammatory responses in COPD progression. Further exploration of SHP2-targeted interventions may offer novel strategies for managing COPD and attenuating disease severity.

### **COMPETING INTERESTS**

The authors report no conflict of interest.

### **FUNDING**

None.

#### **AVAILABILITY OF DATA AND MATERIALS**

The data that support the findings of this study are available from the corresponding author upon

#### **REFERENCES**

- Zhang M-Y, Jiang Y-X, Yang Y-C, et al. Cigarette smoke extract induces pyroptosis in human bronchial epithelial cells through the ROS/NILRP3/caspase-1 pathway. [J]. Life Sci. 2021;269:119090. doi:10.1016/j.fis.2021.119090
- Guan R, Wang J, Cai Z, et al. Hydrogen sulfide attenuates cigarette smoke-induced airway remodelingbyupregulatingSIRT1signalingpathway. [J]. Redox Biol. 2020;28:101356. doi:10.1016/j. redox.2019.101356
- Langen RCJ, Korn SH, Wouters E F M. ROS in the local and systemic pathogenesis of COPD.
   [J]. Free Radic Biol Med. 2003;35(3):226-235. doi:10.1016/S0891-5849(03)00316-2
- Luo Y, Liu LM, Xie L, et al. Activation of the CaR-CSE/H2S pathway confers cardioprotection against ischemia-reperfusion injury. [J]. Exp Cell Res. 2021;398(2):112389. doi:10.1016/j. yexcr.2020.112389
- Achen D, Fernandes D, Kemigisha E, Rukundo GZ, Nyakato VN, Coene G. Trends and Challenges in Comprehensive Sex Education (CSE) Research in Sub-Saharan Africa: a Narrative Review. [J]. Curr Sex Health Rep. 2023;\*\*:1-9. doi:10.1007/s11930-023-00362-1
- McGuinness AJ, Sapey E. Oxidative Stress in COPD: Sources, Markers, and Potential Mechanisms. [J]. J Clin Med. 2017;6(2):21. doi:10.3390/jcm6020021
- Sun L, Ma W, Gao W, et al. Propofol directly induces caspase-1-dependent macrophage pyroptosis through the NLRP3-ASC inflammasome. [J]. Cell Death Dis. 2019;10(8):542. doi:10.1038/s41419-019-1761-4
- Asmamaw MD, Shi XJ, Zhang LR, Liu HM. A comprehensive review of SHP2 and its role in cancer. [J]. Cell Oncol (Dordr). 2022;45(5):729-753. doi:10.1007/s13402-022-00698-1
- Liu Q, Qu J, Zhao M, Xu Q, Sun Y. Targeting SHP2 as a promising strategy for cancer immunotherapy. [J]. Pharmacol Res. 2020;152:104595. doi:10.1016/j.phrs.2019.104595
- Guo W, Liu W, Chen Z, et al. Tyrosine phosphatase SHP2 negatively regulates NLRP3 inflammasome activation via ANT1-dependent mitochondrial homeostasis. [J]. Nat Commun. 2017;8(1):2168. doi:10.1038/s41467-017-02351-0
- Chattopadhyay R, Raghavan S, Rao GN. Resolvin D1 via prevention of ROS-mediated SHP2 inactivation protects endothelial adherens junction integrity and barrier function. [J]. Redox Biol. 2017;12:438-455. doi:10.1016/j.redox.2017.02.023
- Wu YF, Li ZY, Dong LL, et al. Inactivation of MTOR promotes autophagy-mediated epithelial injury in particulate matter-induced airway inflammation. [J]. Autophagy. 2020;16(3):435-450. doi:10.1080/15548627.2019.1628536
- Sun XW, Lin YN, Ding YJ, et al. Surfaxin attenuates PM2.5-induced airway inflammation via restoring surfactant proteins in rats exposed to cigarette smoke. [J]. Environ Res. 2022;203:111864. doi:10.1016/j.envres.2021.111864
- Yu X, Ren LP, Wang C, et al. Role of X-Box Binding Protein-1 in Fructose-Induced De Novo Lipogenesis in HepG2 Cells. [J]. Chin Med J (Engl). 2018;131(19):2310-2319. doi:10.4103/0366-6999.241799
- Fan X, Dong T, Yan K, Ci X, Peng L. PM2.5 increases susceptibility to acute exacerbation of COPD via NOX4/Nrf2 redox imbalance-mediated mitophagy. [J]. Redox Biol. 2023;59:102587. doi:10.1016/j.redox.2022.102587
- Qiu Z, He Y, Ming H, Lei S, Leng Y, Xia ZY. Lipopolysaccharide (LPS) Aggravates High Glucoseand Hypoxia/Reoxygenation-Induced Injury through Activating ROS-Dependent NLRP3 Inflammasome-Mediated Pyroptosis in H9C2 Cardiomyocytes. [J]. J Diabetes Res. 2019;2019:8151836. doi:10.1155/2019/8151836
- Xie Q, Gao S, Lei M, Li Z. Hesperidin suppresses ERS-induced inflammation in the pathogenesis of non-alcoholic fatty liver disease. [J]. Aging (Albany NY). 2022;14(3):1265-1279. doi:10.18632/ aging.203817
- Wang Q, Bu Q, Liu M, et al. XBP1-mediated activation of the STING signalling pathway in macrophages contributes to liver fibrosis progression. [J]. JHEP Rep Innov Hepatol. 2022;4(11):100555. doi:10.1016/j.jhepr.2022.100555
- Tanaka Y, Chen ZJ. STING specifies IRF3 phosphorylation by TBK1 in the cytosolic DNA signaling pathway. [J]. Sci Signal. 2012;5(214):ra20. doi:10.1126/scisignal.2002521
- Fischer FA, Mies L F M. NIZAMI S, et al. TBK1 and IKKε act like an OFF switch to limit NLRP3
  inflammasome pathway activation [J]. Proceedings of the National Academy of Sciences of the
  United States of America, 2021, 118(38).